A novel approach for the intravenous delivery of leuprolide using core-cross-linked polymeric micelles

Qizhi Hu [a,b], Ethlinn V.B. van Gaal [b], Paul Brundel [b], Hans Ippel [c], Tilman Hackeng [c], Cristianne J.F. Rijcken [b], Gert Storm [a,d], Wim E. Hennink [d], Jai Prakash [a,*]

[a] Department of Biomaterials Science and Technology, section: Targeted Therapeutics, MIRA Institute for Biomedical Technology and Technical Medicine, University of Twente, Enschede, The Netherlands
[b] Cristal Therapeutics, Maastricht, The Netherlands
[c] Department of Biochemistry and CARIM, University of Maastricht, Maastricht, The Netherlands
[d] Department of Pharmaceutics, Utrecht Institute for Pharmaceutical Sciences, Utrecht University, Utrecht, The Netherlands

ARTICLE INFO

ABSTRACT

Therapeutic peptides are highly attractive drugs for the treatment of various diseases. However, their poor pharmacokinetics due to rapid renal elimination limits their clinical applications. In this study, a model hormone peptide, leuprolide, was covalently linked to core-cross-linked polymeric micelles (CCL-PMs) via two different hydrolysable ester linkages, thereby yielding a nanoparticulate system with tuneable drug release kinetics. The ester linkage that provided the slowest peptide release kinetics was selected for in vivo evaluation. Compared to the soluble peptide, the leuprolide-entrapped CCL-PMs showed a prolonged circulation half-life (14.4 h) following a single intravenous injection in healthy rats and the released leuprolide was detected in blood for 3 days. In addition, the area under the plasma concentration–time curve (AUC) value was >100-fold higher for leuprolide-entrapped CCL-PMs than for soluble leuprolide. Importantly, the released peptide remained biologically active as demonstrated by increased and long-lasting plasma testosterone levels.
This study shows that covalent linkage of peptides to CCL-PMs via hydrolytically sensitive ester bonds is a promising approach to achieving sustained systemic levels of peptides after intravenous administration.

© 2015 Elsevier B.V. All rights reserved.

1. Introduction

Over the past decades, peptides have emerged as promising therapeutic agents for the treatment of cancer, metabolic disorders, cardiovascular and a variety of other society-burdening diseases [1]. Compared to other biologics (e.g., antibodies), peptides have many advantages such as higher potency, less immunogenicity and easier synthesis and modification [2–4]. However, the development of therapeutic peptides for clinical application still faces substantial challenges. To mention, peptides generally have poor pharmacokinetics. Due to their small molecular size, peptides are rapidly eliminated through the kidneys leading to their short plasma half-life, typically ranging from few hours to minutes [5]. For this reason, frequent dosing is required to achieve therapeutic effects. Moreover, peptides are also susceptible to proteolytic degradation which renders them ineffective [5].

To overcome these limitations of therapeutic peptides, various delivery systems have been developed to enhance the efficacy of peptides through the improvement of their pharmacokinetics and biodistribution profile [6]. For example, the circulation kinetics of peptides can be improved through conjugation to polymers (e.g., polyethylene glycol, polysialic acid), oligosaccharides (e.g., cyclodextrins) or proteins (e.g., human serum albumin) [7–10]. Besides chemical conjugation, peptides can also be noncovalently incorporated into biodegradable long-acting release matrices, such as poly(D,L-lactide-co-glycolide) (PLGA) microparticles, which protects them against degradation and allows their sustained release [6,11]. To maintain prolonged therapeutically relevant plasma levels of peptides (essential for e.g., peptide hormones), peptide formulations are often administered via the subcutaneous (s.c.) or intramuscular (i.m.) route. Such routes of administration allow sustained release of peptides from the locally administered formulations leading to prolonged systemic exposure to the peptide. In the present study, we propose a novel approach for obtaining sustained plasma levels of a peptide by attaching the peptide via a hydrolytically sensitive bond to long-circulating core-cross-linked polymeric micelles (CCL-PMs) after intravenous (i.v.) administration.

Polymeric micelles are self-assembled colloidal particles composed of amphiphilic block copolymers. Their size, typically <100 nm, depends on the molecular weight and the characteristics of the amphiphilic block copolymers [12,13]. Owing to the steric stability provided by the hydrophilic shell and their small size, polymeric micelles can circulate in

* Corresponding author at: Department of Biomaterials Science and Technology, University of Twente, Drienerlolaan 5, Enschede, The Netherlands.
E-mail address: j.prakash@utwente.nl (J. Prakash).

blood for extended periods by evading the mononuclear phagocytic system (MPS) and yet not excreted by kidneys [14–18]. Several polymeric micellar formulations have undergone clinical evaluations as recently reviewed by Cabral et al. [19]. However, a major challenge for polymeric micelles after i.v. administration is their poor in vivo stability as a result of dilution and adsorption of unimers to plasma proteins (e.g., albumin and lipoproteins) [15,20]. To stabilize polymeric micelles for in vivo applications block copolymers can be cross-linked in the micellar core [21, 22]. Furthermore, instead of physical encapsulation, drugs can be covalently entrapped in polymeric micelles to prevent premature drug release from the micelles [23–25].

In this study, CCL-PMs were explored to prevent the rapid renal elimination of therapeutic peptides and to slowly release these peptides in the systemic circulation. Previously, micellar systems based on block copolymers of poly(ethylene glycol) (PEG) and poly(N-(2-hydroxypropyl)methacrylamide-oligolactates) (pHPMAmLac$_n$) have been successfully applied to target dexamethasone and the anticancer drug doxorubicin for the treatment of rheumatoid arthritis and tumours in animals, respectively [23,24,26]. Using this technology, in the present study a model peptide (leuprolide) was covalently linked to CCL-PMs via hydrolysable linkers.

Leuprolide is a potent agonistic analogue of gonadotropin releasing hormone (GnRH), which inhibits the secretion of pituitary gonadotropin and suppresses testicular and ovarian steroidogenesis when administered at therapeutic doses [27,28]. Interestingly, short-term use of leuprolide stimulates pituitary gonadotropin release and briefly increases testosterone levels, while long-term administration induces inhibition of the pituitary-gonadal axis due to down-regulation of the GnRH pituitary receptors leading to reduced systemic testosterone levels and so-called 'chemical castration' in men [29]. However, leuprolide in its free form is rapidly cleared from the bloodstream following parenteral administration, with a biological half-life of ~3 h in healthy male volunteers [30]. The use of CCL-PMs aims to prevent the rapid elimination of leuprolide and achieve sustained bioactive leuprolide levels in the systemic circulation.

In the present study, leuprolide was covalently linked to the micellar core via two different hydrolysable linkages based on either a sulfide or a sulfoxide ester. The in vitro release profiles of both micellar dispersions were compared, and the leuprolide-entrapped CCL-PMs with the slower release kinetics was selected for in vivo assessment. The pharmacokinetic profile of the selected leuprolide-entrapped CCL-PMs was evaluated in healthy rats. Furthermore, the bioactivity of released peptide from these leuprolide-entrapped CCL-PMs was determined by measuring plasma testosterone levels.

2. Materials and methods

2.1. Materials

Leuprolide HCl (pGlu-His-Trp-Ser-Tyr-Leu-Leu-Arg-Pro-NHC$_2$H$_5$, molecular mass 1209.5 Da) and the internal standard for leuprolide (pGlu-His-Trp-Ser-Tyr-Ala-Leu-Arg-ProNHC$_2$H$_5$) were obtained from Bachem AG (Bubendorf, Switzerland). Testosterone-17β (androst-4-ene-17β-ol-3-one) and internal standard testosterone-17β-d3 were obtained from Steraloids (Newport, RI) and CDN-Isotopes (Quebec, Canada) respectively. N,N′-dicyclohexylcarbodiimide (DCC), 4-dimethylaminopyridine (DMAP), 4-methoxyphenol, methacrylic anhydride, potassium persulfate (KPS), tetramethylethylenediamine (TEMED), trifluoroacetic acid (TFA), ammonium acetate and formic acid were purchased from Sigma Aldrich (Zwijndrecht, The Netherlands). N,N-dimethylformamide (DMF) and acetonitrile (ACN) were purchased from Biosolve (Valkenswaard, The Netherlands). Triethylamine (TEA) was purchased from Merck (Darmstadt, Germany). The monomers N-2-hydroxypropyl methacrylamide monolactate (HPMAmLac$_1$) and N-2-hydroxypropyl methacrylamide dilactate (HPMAmLac$_2$) as well as the

initiator (mPEG$_{5000}$)$_2$-ABCPA were synthesized as described previously [31]. The other chemicals were used as received.

2.2. Synthesis and analysis of leuprolide-derivatives

2.2.1. Synthesis of leuprolide-L1

2-((2-(Methacryloyloxy)ethyl)thio) acetic acid (L1) was synthesized as described previously [24] (Fig. 1A). Next, leuprolide was conjugated to L1 as illustrated in Fig. 1B. In brief, leuprolide (0.12 mmol), L1 (0.30 mmol) and DMAP (0.30 mmol) were dissolved in 3.7 mL DMF. Subsequently, DCC (0.33 mmol) was added and the resulting mixture was stirred for 16 h at room temperature. Next, the reaction mixture was filtered and then evaporated at 45 °C under reduced pressure. The residual oil was purified using preparative HPLC (Agilent 1100/1200 integrated with Waters Sunfire Prep C18 5 μm OBD 30 × 50 mm column; eluent A: 95% H$_2$O/5% ACN/0.1% formic acid; eluent B: 5% H$_2$O/95% ACN/0.1% formic acid) and freeze-dried to obtain leuprolide-L1 (LeuL1) as fluffy white powder.

2.2.2. Synthesis of leuprolide-L2

2-((2-(Methacryloyloxy)ethyl) sulfinyl)acetic acid (L2) was synthesized essentially as previously described with minor modifications [24] (Fig. 2A). In brief, compound 2 (5.12 mmol) was dissolved in ACN (18 mL) and mixed with a solution of sodium periodate (7.68 mmol) in H$_2$O (18 mL). The reaction mixture was stirred for 16 h at room temperature and then filtered. The filtrate was extracted three times with ethyl acetate. The combined organic layers were washed with brine, dried over Na$_2$SO$_4$ and evaporated to dryness to obtain an oil which solidified upon standing. The resulting solid was dissolved in diethyl ether (50 mL) and cooled to −40 °C. The obtained precipitate was filtered, washed with cold diethyl ether and dried to obtain compound 3 (61% yield) as a white solid. Next, compound 3 (4.67 mmol) and a trace amount of 4-methoxyphenol (to prevent premature polymerization) were dissolved in cold TFA (2.95 mL) under nitrogen and stirred in an ice bath for 2 h. Thereafter, TFA was removed by evaporation in vacuo and coevaporation with toluene. The resulting yellow oil was stirred with diethyl ether (20 mL) for 15 min and the precipitate was filtered to obtain L2 as a white solid (38% yield). Subsequently leuprolide was conjugated to L2 to obtain leuprolide-L2 (LeuL2) using the same method as described in Section 2.2.1. (Fig. 2B).

2.2.3. Analysis of leuprolide derivatives

The molecular mass of leuprolide derivatives was determined using electrospray ionization mass spectrometry (ESI-MS) on a Shimadzu liquid chromatography–mass spectrometry (LC–MS) QP8000 in positive ion mode. A Gemini® 3 μm C18 column (150 × 3 mm) (Phenomenex) was used with a gradient from 100% eluent A (95% H$_2$O/5% ACN/0.1% TFA) to 100% B (5% H$_2$O/95% ACN/0.1% TFA) in one hour with a flow of 1 mL/min and UV-detection at 253 nm. The mass used to identify leuprolide-L1 and leuprolide-L2 was m/z 1396 (M + H)$^+$ and m/z 1412 (M + H)$^+$, respectively.

The synthesized leuprolide derivatives were measured by nuclear magnetic resonance (NMR) spectroscopy on a Bruker AVANCE III HD 700 MHz spectrometer equipped with a TCI cryoprobe, using DMSO-d6 as solvent. For each leuprolide derivative, the numbering scheme of the linker is given in Supplementary Fig. 1 and a full NMR characterisation was carried out by applying various homo- and heteronuclear two-dimensional experiments to obtain complete sets of ^{1}H, ^{15}N and ^{13}C resonance assignments (Supplementary Table S1–S3).

2.3. Synthesis of mPEG$_{5000}$-b-pHPMAmLac$_n$ block copolymer

Block copolymer containing a hydrophilic block of monomethoxy poly(ethylene glycol) (mPEG, M$_n$ = 5000) and a thermosensitive block composed a random copolymer of HPMAmLac$_1$ and HPMAmLac$_2$ (Fig. 3) was synthesized. The feed molar ratio of HPMAmLac$_1$: HPMAmLac$_2$ was
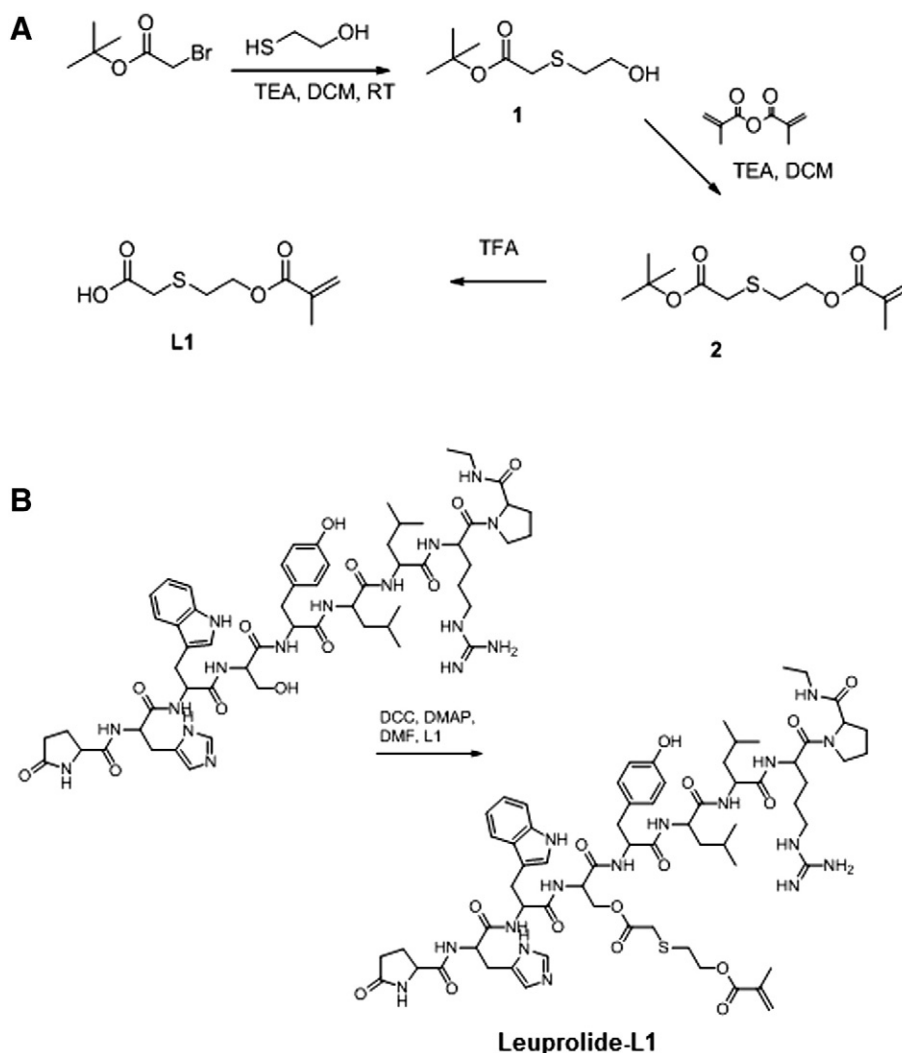
Fig. 1. Synthesis of leuprolide-L1. (A) Synthesis scheme of L1 [24] and (B) conjugation of L1 to leuprolide.

53/47. The block copolymer was prepared by free radical polymerization using (mPEG$_{5000}$)$_2$-ABCPA as initiator (molar ratio of monomer: initiator was 150:1) as described previously [20,32]. Subsequently, 13 mol% of the lactate side chains was derivatized with methacrylate groups upon reaction with methacrylic anhydride according to a protocol reported previously [20]. The obtained block copolymer was characterised using methods described elsewhere [23,33].

2.4. Preparation of leuprolide-entrapped CCL-PMs

Polymeric micelles were formed using the fast heating method [34]. In brief, an ice-cold solution of methacrylated mPEG-b-pHPMAmLac$_n$ block copolymer (830 μL, 24 mg/mL) was mixed with TEMED (25 μL, 120 mg/mL) dissolved in ammonium acetate 150 mM pH 5.0 buffer. Subsequently, LeuL1 or LeuL2 (100 μL, 20 mg/mL leuprolide equiv., dissolved in 50/50 (v/v) ethanol/water mixture) was added, followed by rapid heating to 60 °C while stirring vigorously for 1 min to form polymeric micelles. The micellar dispersion was then transferred into a vial containing KPS (45 μL, 30 mg/mL). The polymeric micelles were covalently stabilized by crosslinking the methacrylate moieties of both the leuprolide derivatives as well as the polymers under a N$_2$ atmosphere for 1 h at RT, to obtain either LeuL1-entrapped CCL-PMs (LeuL1 CCL-PMs) or LeuL2-entrapped CCL-PMs (LeuL2 CCL-PMs) (Fig. 3). The final concentrations of block copolymer and leuprolide derivatives (leuprolide equivalents) were 20 and 2 mg/mL, respectively. Next, the LeuL1 CCL-PMs and

LeuL2 CCL-PMs dispersions were filtered using 0.2 μm cellulose membrane filters to remove large particles/aggregates.

For the in vivo study, LeuL1 CCL-PMs were purified and concentrated 5 times using a KrosFlo Research IIi Tangential Flow Filtration (TFF) System equipped with modified polyethersulfone (mPES) MicroKros® filter modules (MWCO 500 kDa). Ammonium acetate 20 mM pH 5.0 buffer containing 130 mM NaCl was used as the washing buffer and referred to as "vehicle" in the following sections.

2.5. Particle size distribution

The size of LeuL1 and LeuL2 CCL-PMs was measured by dynamic light scattering (DLS) using a Malvern ALV/CGS-3 Goniometer. DLS results are given as a z-average particle size diameter (Z_{ave}) and a polydispersity index (PDI).

2.6. Transmission electron microscopy (TEM)

Transmission electron microscopy (TEM) analysis of the different micellar dispersions was conducted using a Philips Tecnai 12 microscope equipped with a Biotwin-lens and a LaB6 filament, operated at 120 kV acceleration voltage. Glow discharged grids (copper 200 mesh grid with a carbon-coated thin polymer film, Formvar on top) were used for sample preparation and 2% uranyl acetate (w/v) was used as
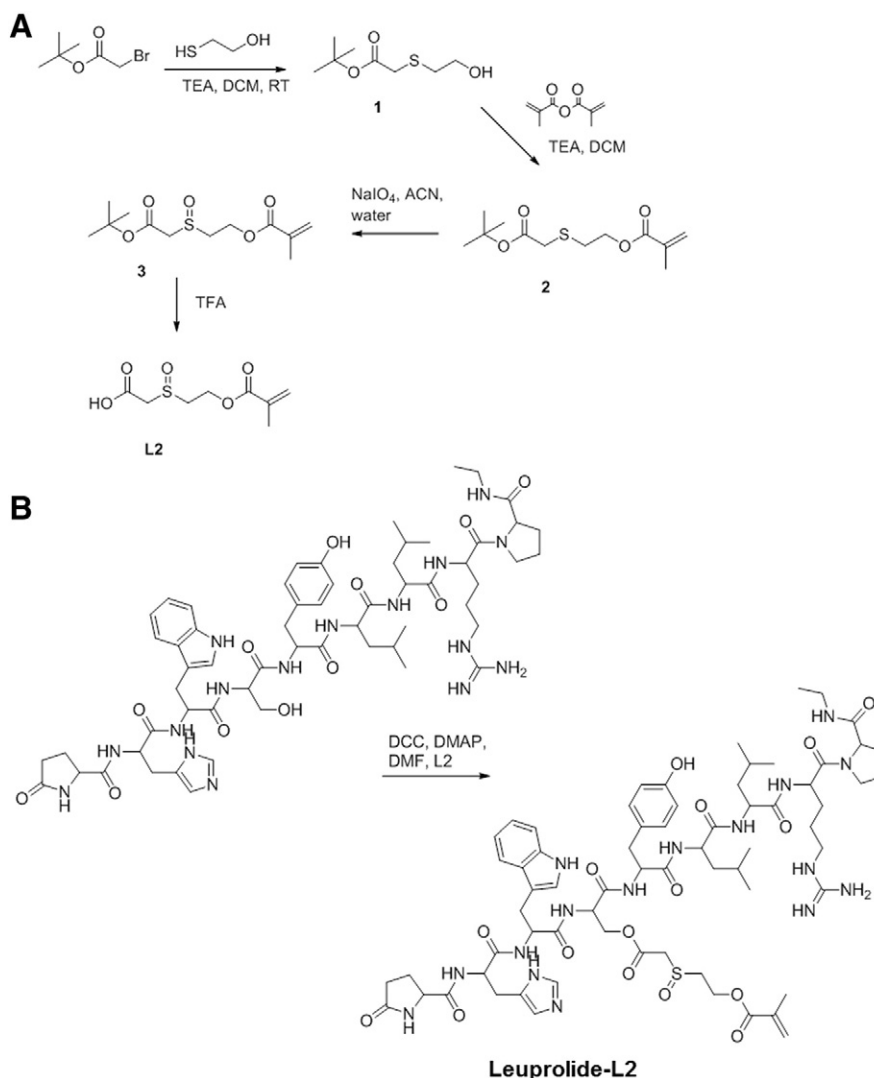
Fig. 2. Synthesis of leuprolide-L2. (A) Synthesis scheme of L2 and (B) conjugation of L2 to leuprolide.

a negative stain. Images were captured with a SIS Megaview II CCD camera and processed with AnalySIS software.

2.7. Determination of free and total leuprolide content

The concentration of free leuprolide, free leuprolide-L1 or leuprolide-L2 in the micellar dispersions was determined by ultra-performance liquid chromatography (UPLC) (Waters, USA) using an Acquity BEH C18 1.7 μm column (50 × 2.1 mm) (Waters). A gradient from 100% eluent A (95% H_2O/5% ACN/0.1% formic acid) to 100% B (10% H_2O/90% ACN/0.1% formic acid) was used at a flow of 0.25 mg/mL. The injection volume was 7 μL and the runtime was 5 min. The determination was performed using an ultraviolet/visible light detector (TUV, Waters) set at 210 nm. Leuprolide dissolved in water was used for calibration.

Prior to injection, LeuL1 CCL-PMs or LeuL2 CCL-PMs were diluted 10-fold in ammonium acetate 150 mM pH 5.0 buffer and stored at 5 °C to minimize additional hydrolysis.

The concentration of total (entrapped and released) leuprolide in the micellar dispersions was determined by measurement of released leuprolide upon hydrolysis of the ester bonds in borate 100 mM pH 9.4 buffer supplemented with NaCl to isotonicity at 37 °C. The release was considered complete when a plateau in leuprolide concentration was

reached. The concentration of total leuprolide was measured by UPLC using the same analytical method mentioned above.

The amount of peptide entrapped is calculated as follows: amount of peptide entrapped = amount of total leuprolide content – amount of free leuprolide – amount of free leuprolide derivative (leuprolide equiv.). The peptide entrapment efficiency (EE) and peptide loading (PL) were calculated using the UPLC data as follows:

$$EE = \frac{\text{Amount of peptide entrapped}}{\text{Amount of peptide added}} \times 100\%.$$

$$PL = \frac{\text{Amount of peptide entrapped}}{\text{Amount of (peptide entrapped + polymer added)}} \times 100\%.$$

2.8. In vitro leuprolide release from CCL-PMs

The in vitro release of leuprolide from CCL-PMs was measured in phosphate buffered saline pH 7.4 at 37 °C. Briefly, LeuL1 CCL-PMs or LeuL2 CCL-PMs dispersions (prepared using the methods described in Section 2.4) were diluted 40-fold in phosphate 100 mM pH 7.4 buffer supplemented with 15 mM NaCl (max. 50 μg/mL leuprolide equiv.). The concentration of released leuprolide was determined by UPLC
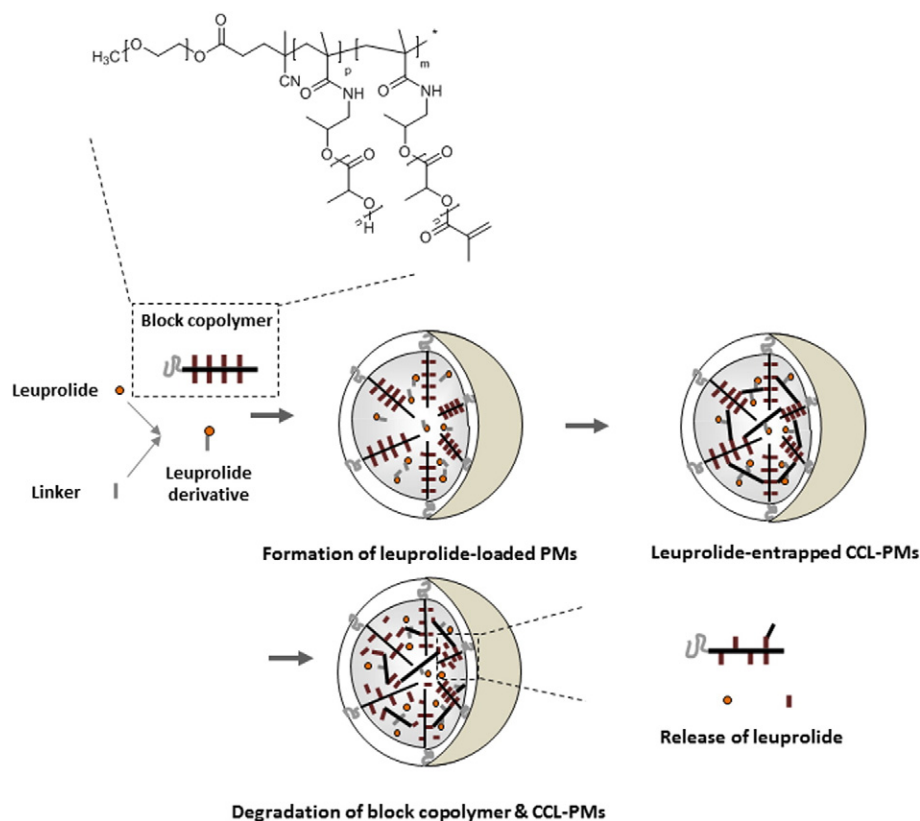
Fig. 3. Synthesis scheme of leuprolide-entrapped CCL-PMs.

using the analytical method mentioned in Section 2.7. The percentage of leuprolide release is calculated as:

$$\% \text{ Release of leuprolide} = \frac{\text{Amount of released leuprolide}}{\text{Amount of total leuprolide}} \times 100\%.$$

2.9. Pharmacokinetics

Animal experiments were conducted in compliance with the national regulations and approved by the local ethical committee for animal experimentation. Fifteen male Sprague Dawley rats (Charles River Deutschland, Germany) weighing ~300 g were randomly divided into five groups of three rats. All animals were housed in a temperature-controlled room (21 ± 3 °C), with 55 ± 15% relative humidity, and a photoperiod of 12/12 h. Tap-water and pelleted rodent food (SM R/M-Z from SSNIFF® Spezialdiäten GmbH, Germany) were provided to the animals.

Leuprolide dissolved in ammonium acetate 20 mM pH 5.0 buffer also containing 130 mM NaCl (referred to as "soluble leuprolide") was injected i.v. into the tail vein of the rats at a dose of 0.10 mg/kg. We selected LeuL1 CCL-PMs for the in vivo studies considering the peptide release profile as explained in the result and discussion section. Dispersions of LeuL1 CCL-PMs were injected i.v. into the tail vein of the rats at doses of 0.13, 1.3 and 13 mg/kg leuprolide, respectively. As a control group, the vehicle itself was injected i.v. into the rats. Blood samples (approximately 0.5 mL per sampling time point) were serially collected in tubes containing K₃-EDTA from the vena cava via a cannula which was inserted into the jugular vein. Within 30 min after sampling, the blood samples were centrifuged and the plasma samples were stored at −75 °C until analysis. The concentrations of released and total (released plus entrapped) leuprolide as well as endogenous testosterone-17β in plasma were determined using the method described in the following section.

2.10. Determination of released leuprolide, total leuprolide and endogenous testosterone-17β concentrations in rat plasma

Released and total (released plus entrapped) leuprolide as well as endogenous testosterone-17β concentrations in rat plasma were determined by LC-MS. Prior to the extraction procedure of the samples, the internal standards pGlu-His-Trp-Ser-Tyr-Ala-Leu-Arg-Pro-NHC₂H₅ and testosterone-17β-d3 were added to 100 μL of rat plasma for the quantification of leuprolide and testosterone-17β, respectively. For the determination of released leuprolide and testosterone-17β concentrations, the rat plasma samples were diluted 1:1 with ammonium acetate 150 mM pH 5.0 buffer. For the determination of total leuprolide concentration, rat plasma samples were 1:1 diluted with borate 100 mM pH 9.4 buffer supplemented with NaCl to isotonicity and incubated at 37 °C for 48 h to ensure full release of leuprolide. Next, ice-cold acetonitrile (2 × 200 μL) was added stepwise to the plasma, followed by brief vortexing. The samples were subsequently centrifuged (12,000 ×g) for 8 min and the supernatants were evaporated in a SpeedVac until dryness. Next, the residue was dissolved in 40 μL of solvent (50% ACN in water with 0.1% formic acid).

The samples were subsequently analysed by LC-MS using a Dionex Ultimate 3000 RSLC system equipped with a NCS-3500RS binary nanoLC pump and VWD-3400RS variable wavelength detector (Dionex Softron GmbH, Germering, Germany). Chromatographic separation was achieved on an Eclipse Plus C18 column (1.8 μm, 2.1 × 50 mm) from Agilent (Waldbronn, Germany) at a flow rate of 0.3 mL/min. The mobile phase consisted of eluent A (90% H₂O/10% ACN/0.1% formic acid (v/v)/2 mM ammonium acetate) and eluent B (10% H₂O/90% ACN/0.1% formic acid (v/v)/2 mM ammonium acetate) and the injection volume was 10 μL. Mass spectrometric detection was performed on an Agilent 6540 Q-TOF Accurate Mass spectrometer (Agilent Technologies, Santa Clara, CA), which operated in the positive ion mode using a Jet Stream electrospray ionization (ESI) source. The masses used to identify and quantify the analytes were m/z 605.3300 (M + 2H)²⁺ for leuprolide, m/z 584.3065

Table 1
Characteristics of (methacrylated) mEPG5000-b-pHPMAmLacn block copolymer.

M_w (kg/mol)	PD (M_w/M_n)	M_n of pHPMAmLac$_n$ (kg/mol)	M %	Critical micelle temperature (°C)
31.6	2.5	15.0	12	10

The M_w and polydispersity (PD) of the (methacrylated) block copolymers were determined by GPC; the number average molecular weight (M_n) of the thermosensitive block of the block copolymer and percentage of methacrylation (M %) were determined by ^{1}H NMR analysis; the critical micelle temperature of the methacrylated block copolymer was determined by UV–VIS spectrophotometer, essentially as described previously [38].

$(M + 2H)^{2+}$ for internal standard leuprolide (pGlu-His-Trp-Ser-Tyr-Ala-Leu-Arg-Pro-NHC$_2$H$_5$), m/z 289.2162 $(M + H)^+$ for testosterone-17β and m/z 292.2350 $(M + H)^+$ for testosterone-17 β-d3.

2.11. Statistical analysis

Pharmacokinetic data are presented as the mean ± SD of 3 rats per group unless otherwise noted. Pharmacokinetic parameters were calculated using Multifit pharmacokinetic software (University of Groningen, The Netherlands) by a two compartment nonlinear model as described previously [35]. Statistical significance was analysed using two-tailed unpaired Student's t-test. A p-value < 0.05 was considered statistically significant. The linear correlation between AUC∞ and administered leuprolide dose was tested using an unpaired two-tailed Student's t-test.

3. Results and discussion

3.1. Synthesis and purification of leuprolide derivatives

L1 or L2 was conjugated to leuprolide through DCC/DMAP mediated esterification of the carboxyl group of the linker and the hydroxyl group of serine residue of the peptide, thereby yielding methacrylated leuprolide derivatives containing either a sulfide (LeuL1) or a sulfoxide (LeuL2) ester.

LeuL1 and LeuL2 were purified by prep-HPLC and obtained in 42% and 27% yields, respectively. As evidenced by LC–MS analysis, only one linker molecule was conjugated to leuprolide as peaks for LeuL1 and LeuL2 were observed at m/z 1394 $(M + H)^+$ and m/z 1410 $(M + H)^+$, respectively (Supplementary Fig. 2). As shown in Table S1, the ^{1}H chemical shifts of the serine residue in leuprolide derivatives significantly differed from those observed in leuprolide [36], indicating that the linker was conjugated at the hydroxyl group of serine residue. Evidence for the covalent attachment follows directly from the observed ^{1}H–^{1}H NOE contacts going from serine sidechain protons to methylene (H1) protons in the linker, as well as the presence of long-range ^{1}H–^{13}C couplings between serine beta protons and the adjacent C=O carbonyl carbon (C8) of the linker. To mention, the ^{1}H chemical shifts of tyrosine residue in leuprolide derivatives were in good agreement with those observed in leuprolide [36], suggesting that the tyrosine hydroxyl group was not modified in the conjugation reaction. This selective conjugation also corroborates the findings of Sundaram et al. where the carboxyl group of docetaxel hemiglutarate was selectively conjugated to GnRH agonist deslorelin via the serine hydroxyl group of the peptide (instead of the phenolic hydroxyl group in tyrosine) [37].

3.2. Synthesis and characterisation of mPEG5000-b-pHPMAmLac$_n$ block copolymer

A thermosensitive block copolymer composed of a random block of pHPMAm-Lac$_1$/Lac$_2$ and a hydrophilic mPEG block was prepared via radical polymerization and obtained in good yield (~85%). The critical micelle temperature (CMT) of the synthesized block copolymer was 28 °C. The number average molecular weight of the block copolymer as determined by NMR was ca. 20 kg/mol (Table 1). Gel permeation chromatography (GPC) analysis showed that the block copolymer had an average molecular weight of ca. 32 kg/mol with a polydispersity of 2.5, which is normal for this type of free radical polymerization [23]. In a subsequent step, 12 mol% of the lactate groups of the mPEG-b-p(HPMAmLac$_n$) block copolymer was derivatized with methacrylate groups and the CMT of the methacrylated polymer was 10 °C, which is in good agreement with previous data [23]. The Z-average hydrodynamic diameter and PDI of polymeric micelles composed of the methacrylated block copolymer (2 mg/mL) were 65 nm and 0.04, respectively, which are in line with previous data [33].

3.3. Preparation and characterisation of leuprolide-entrapped CCL-PMs

LeuL1 and LeuL2 were covalently entrapped in CCL-PMs to obtain LeuL1 CCL-PMs and LeuL2 CCL-PMs, respectively. The Z-average hydrodynamic diameters of these CCL-PMs were about 70 nm, with a low PDI (<0.1) (Table 2, Fig. 4A). This particle size is typical for CCL-PMs prepared from this type of block copolymer [24]. The morphology of the LeuL1 CCL-PMs and LeuL2 CCL-PMs was spherical, as demonstrated by TEM analysis (Fig. 4B). After purification and concentration by TFF, the mean particle size and PDI of LeuL1 CCLPMs remained the same. The leuprolide entrapment efficiency was 35% and 40% for LeuL1 and LeuL2 respectively, while free leuprolide, free LeuL1 or LeuL2 content was less than 1%. Considering the high hydrophilicity of LeuL1 and LeuL2 (calculated (c) Log P = 1.08 and 0.15, respectively, calculated using Chemdraw), the entrapment efficiency is surprisingly high, likely due to the covalent linkage that is formed between the peptide and the CCL-PMs. A similar drug entrapment efficiency was also found with doxorubicin covalently entrapped in CCL-PMs [23].

3.4. In vitro leuprolide release from leuprolide-entrapped CCL-PMs

The hydrolysis of the ester bonds linking leuprolide to CCL-PMs allows leuprolide to be released in time. The peptide release profiles of LeuL1 CCL-PMs and LeuL2 CCL-PMs were evaluated under physiological conditions (pH 7.4, 37 °C). Fig. 5 shows that leuprolide was released from the CCL-PMs in a sustained fashion, following first-order kinetics ($R^2 > 0.99$ and $R^2 > 0.96$ for LeuL1-CCL-PMs and LeuL2-CCL-PMs respectively). Importantly, the release of leuprolide from CCL-PMs containing sulfide-ester linked leuprolide (LeuL1, $t_{1/2} = 3.7 \pm 0.2$ days) was much slower than that from CCL-PMs containing the sulfoxide-ester linked leuprolide (LeuL2, $t_{1/2} = 0.9 \pm 0.1$ day). Compared to LeuL1, LeuL2 has a higher degree of oxidation of sulfur and therefore a reduced electron density at the carbonyl group of the ester bond. This in turn results in a faster hydrolysis of the ester bond in sulfoxide ester and thereby faster release of leuprolide from LeuL2 CCL-PMs. These data demonstrate that the release kinetics of leuprolide can be tailored by employing linkers
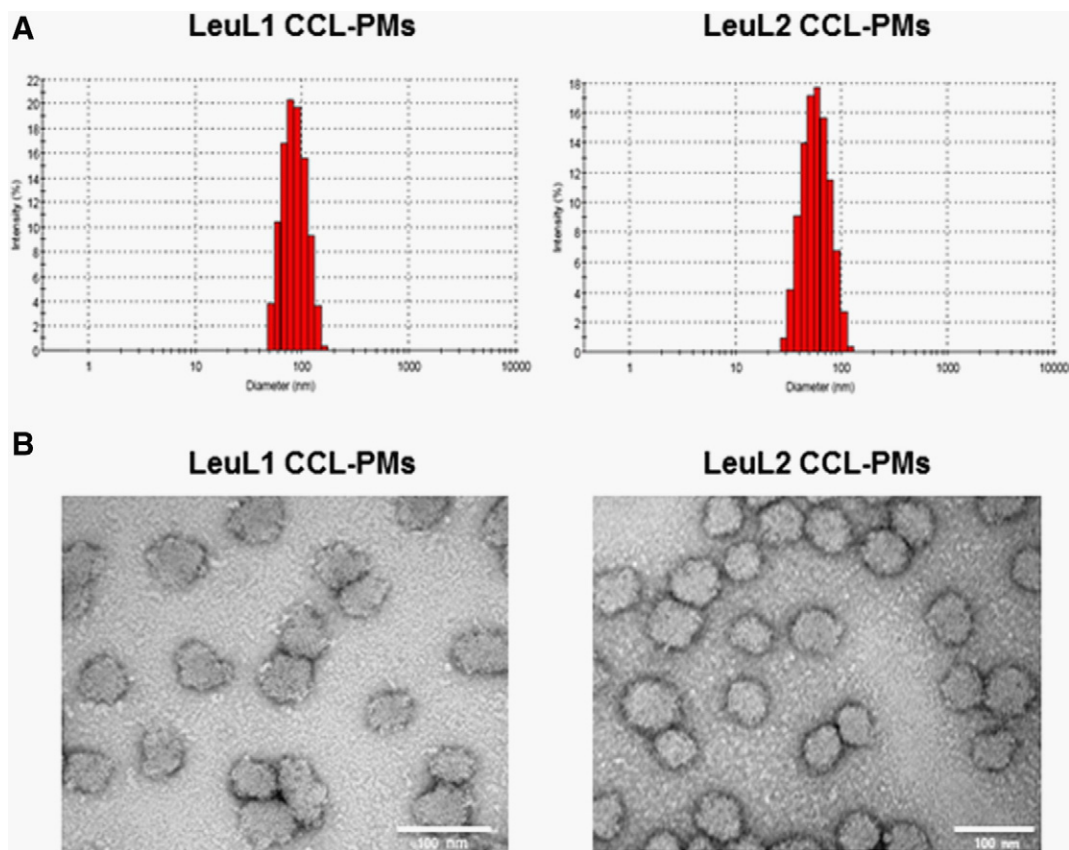
Table 2
Characterisation of LeuL1 CCL-PMs and LeuL2 CCL-PMs.

	Z-average hydrodynamic diameter (nm)	PDI	EE (%)	PL (%)	Free leuprolide (%)	Free leuprolide derivative (%)
LeuL1 CCL-PMs	74 ± 7	0.03 ± 0.02	35 ± 3	3.3 ± 0.3	<1%	<1%
LeuL2 CCL-PMs	68 ± 1	0.02 + 0.01	40 ± 8	3.9 ± 0.7	<1%	<1%

Z-average hydrodynamic diameters, polydispersity index (PDI) of LeuL1 CCL-PMs and LeuL2 CCL-PMs were analysed using DLS. The percentage of peptide entrapment efficiency (% EE), peptide loading (% PL) as well as the percentage of free leuprolide and leuprolide derivative in LeuL1 CCL-PMs and LeuL2 CCL-PMs were determined by UPLC analysis. Data are expressed as the mean ± SD of 2–3 different batches.

Fig. 4. Particle size distribution and morphology of LeuL1 CCL-PMs and LeuL2 CCL-PMs. (A) hydrodynamic size distribution and (B) TEM image.

containing thioether esters with different degrees of oxidation (i.e., a sulfide (L1) or sulfoxide (L2) ester), as previously reported by Crielaard et al. for dexamethasone [24].

Leuprolide is a peptide hormone that exerts its therapeutic effect through the suppression of luteinizing hormone (LH) and follicle stimulating hormone (FSH). Thus sustained leuprolide levels are desired in the bloodstream. To achieve this, the linkage that renders the slowest leuprolide release kinetics should be employed. Besides, given a polymeric micelle system with prolonged circulation kinetics, the release rate of peptide should be slow enough to exploit the long
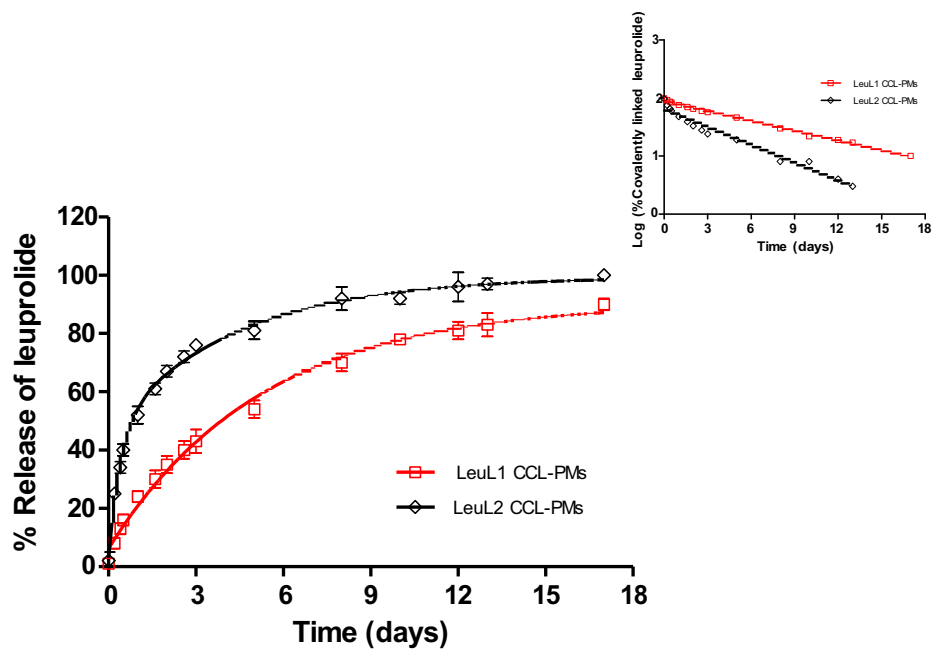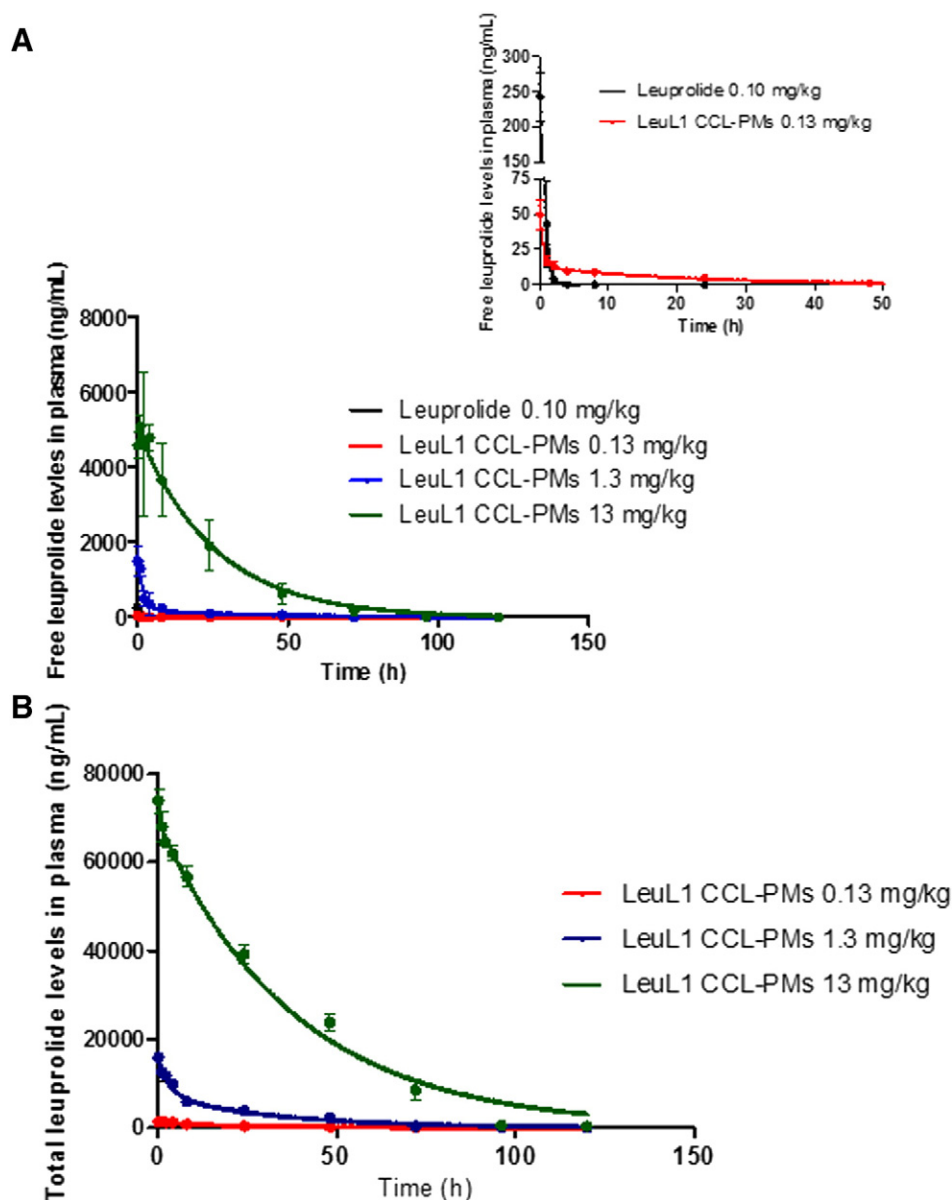

Fig. 5. Release of leuprolide from CCL-PMs with leuprolide covalently linked to the core via two different hydrolysable ester linkages at 37 °C, pH 7.4. Data are expressed as the mean ± SD of 2–3 batches.

Fig. 6. Leuprolide plasma levels after single i.v. administration of leuprolide solution (0.10 mg/kg) or LeuL1 CCL-PMs (0.13 mg/kg, 1.3 mg/kg and 13 mg/kg, respectively) in rats. (A) Released leuprolide plasma levels. (B) Total leuprolide plasma levels. Data are expressed as the mean ± SD (n = 3).

residence of the carrier system as to obtain steady drug plasma levels. Therefore, in our study the micellar dispersion with the slowest peptide release kinetics (i.e., LeuL1 CCL-PMs) was selected for in vivo evaluation.

3.5. Pharmacokinetic profile of LeuL1 CCL-PMs

The pharmacokinetics of leuprolide formulated in either free form or CCL-PMs were evaluated in a rat model. Plasma was obtained at various time points after a single i.v. administration of vehicle, soluble leuprolide and different doses of LeuL1 CCL-PMs. Plasma samples were analysed to determine released and total (released plus entrapped) leuprolide concentrations. The plasma-disappearance curves of released and total leuprolide are shown in Fig. 6 and the calculated pharmacokinetic parameters for LeuL1-CCL-PMs are depicted in Table 3.

As expected, rats treated with vehicle alone (without peptide) showed leuprolide levels below the limit of detection (LOD) (i.e., 0.1 ng/mL) at all the time points. We found that soluble leuprolide (0.1 mg/kg) was rapidly eliminated from the circulation and the plasma levels were detectable only for 2 h post-administration.

Due to the limited time points, pharmacokinetic parameters for soluble leuprolide could not be calculated and are therefore not included in Table 3.

In contrast, LeuL1 CCL-PMs (0.13 mg/kg) drastically extended the blood residence time of released leuprolide (t $_{1/2}$ = 14.4 h),

Table 3

Pharmacokinetic data of total (released plus entrapped) leuprolide in plasma following i.v. administration of LeuL1 CCL-PMs (0.13 mg/kg, 1.3 mg/kg and 13 mg/kg, respectively) in rats. Data are presented as the mean ± standard error (n = 3).

	LeuL1 CCL-PMs 0.13 mg/kg	LeuL1 CCL-PMs 1.3 mg/kg	LeuL1 CCL-PMs 13 mg/kg
$t_{1/2}$ (h)	18.6 ± 29.9	22.6 ± 11.0	26.6 ± 4.0
AUC∞ (h ∗ ng/mL)	26,158 ± 7843	268,877 ± 61,414	2,666,680 ± 338,457
CL (mL/kg/h)	5 ± 1	5 ± 1	5 ± 1
Vss (mL/kg)	113 ± 67	143 ± 38	187 ± 10
MRT (h)	23 ± 19	30 ± 13	38 ± 6

$t_{1/2}$ = half-life of elimination, AUC∞ = area under the plasma concentration–time curve, CL = clearance, Vss = steady-state volume of distribution, MRT = mean residence time.
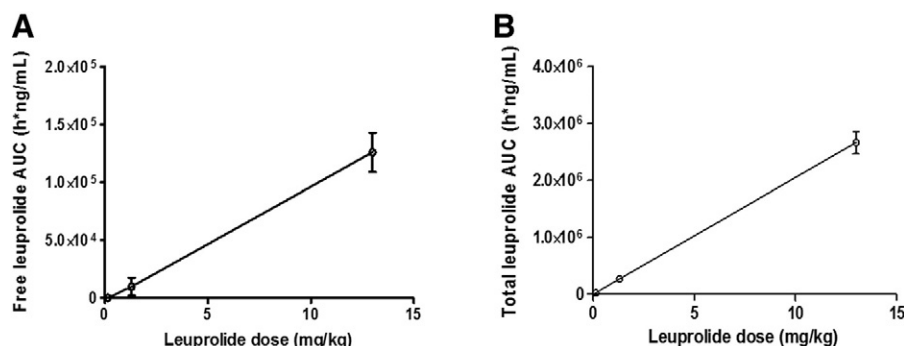
Fig. 7. AUC∞ after i.v. administration of LeuL1 CCL-PMs at three different doses (0.13 mg/kg, 1.3 mg/kg and 13 mg/kg) in rats. (A) Released leuprolide plasma levels. (B) Total leuprolide plasma levels. These data are from the same experiment as that in Fig. 6. Data are expressed as the mean ± SD (n = 3).

which was detected in blood for 3 days (Fig. 6A). This is attributed to the prolonged blood residence of the CCL-PMs [39,40] and covalent peptide conjugation. Accordingly, the AUC∞ of LeuL1 CCL-PMs (26,158 h ∗ ng/mL) was 178-fold higher than the predicted AUC∞ value of soluble leuprolide (147 h ∗ ng/mL). Compared to soluble leuprolide, the i.v. administration of LeuL1 CCL-PMs gave rise to a five-fold lower peak of leuprolide plasma concentration, potentially precluding peak-related side effects. Importantly, the administration of LeuL1 CCL-PMs led to a 2-fold higher plasma AUC∞ of released leuprolide than did soluble leuprolide. The systemic exposure to soluble leuprolide was essentially due to the high peak concentration while sustained plasma levels of released leuprolide was attained with LeuL1 CCL-PM for 3 days (Fig. 6A). As shown with other (similar) systems [20,39,41,42], the small hydrodynamic size and stealth properties provided by PEG chains allow polymeric micelles to escape MPS recognition and subsequent clearance, leading to prolonged circulation time. It may be assumed that while CCL-PMs are circulating in blood, hydrolysis of the sulfide ester occurs, giving rise to the release of leuprolide in the bloodstream in a sustained manner. It is also possible that (part of) leuprolide is released from the micelles upon

uptake by macrophages (e.g., in the liver) and subsequently re-enters the systemic circulation as released leuprolide.

As shown in Fig. 6, the plasma-disappearance curves of released and total leuprolide followed the same pattern after i.v. administration of LeuL1 CCL-PMs at various doses. These data suggest that the leuprolide levels in plasma are dictated by the residence of LeuL1 CCL-PMs in circulation. Moreover, the AUC∞ of both released and total leuprolide plasma levels are correlated linearly with the administered dose of LeuL1-CCL-PMs (released leuprolide level: P = 0.008, R^2 > 0.999; total leuprolide level: P < 0.001, R^2 > 0.999) (Fig. 7). The linear correlation between AUC∞ and the administration dose of LeuL1 CCL-PMs implies a linear bioavailability at a dose between 0.13 and 13 mg/kg. These data demonstrate that the plasma leuprolide levels on demand can be achieved by adjusting the dose proportionally.

As the total leuprolide plasma levels are mainly contributed by the intact LeuL1 CCL-PMs, the observed half-life of elimination ($t_{½}$) of total leuprolide plasma level reflects the circulation half-life of LeuL1 CCL-PMs. Plasma disappearance of LeuL1-CCL-PMs showed log-linear pharmacokinetics for all doses, with a half-life of elimination ($t_{½}$) of
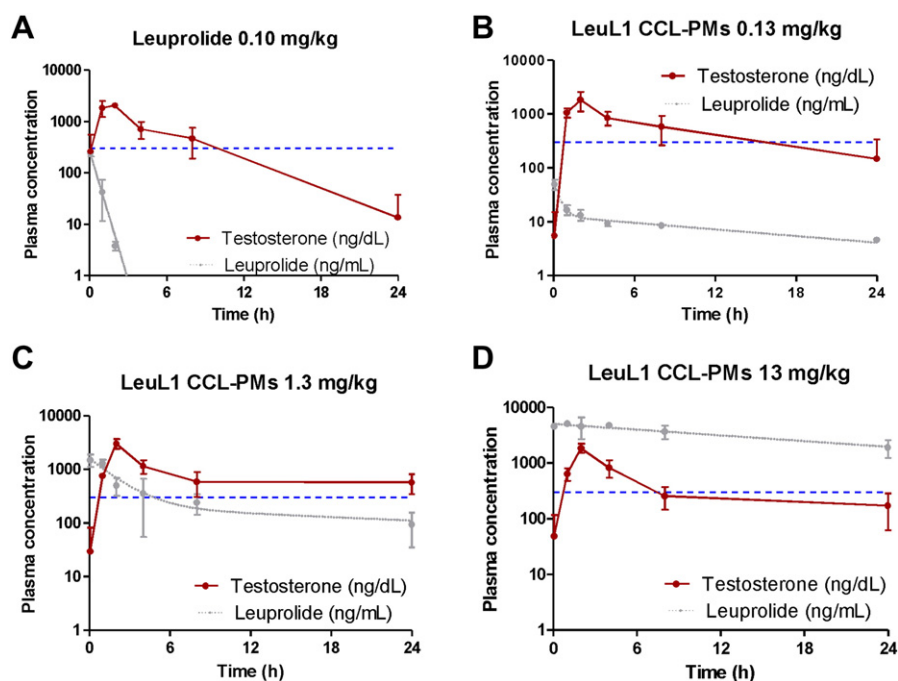
Fig. 8. Testosterone and released leuprolide plasma levels in rats between 0 and 24 h post single i.v. injection of leuprolide solution (0.10 mg/kg) or LeuL1 CCL-PMs (0.13 mg/kg, 1.3 mg/kg and 13 mg/kg, respectively). The blue dashed line indicates the average basal plasma testosterone level in male Sprague–Dawley rats [52]. Released leuprolide levels (grey line) have been shown in Fig. 6A. Data are expressed as the mean ± SD (n = 3).

22.6 ± 4.0 h, indicating dosage-independence of blood clearance of LeuL1 CCL-PMs. This phenomenon has also been observed in PEGylated liposomes [43].

3.6. Testosterone levels in plasma

Both animal and human studies have demonstrated that the administration of leuprolide induces a marked release of hormones LH and FSH in the circulation, which subsequently stimulates an initial and temporary boost in testosterone levels in males [44–47]. Therefore, to establish that leuprolide is released from LeuL1 CCL-PMs in its biologically active form, plasma testosterone levels were determined. As shown in Fig. 8, plasma testosterone levels increased immediately after i.v. administration of soluble leuprolide. Likewise, an increase of testosterone levels was also observed after i.v. administration of LeuL1 CCL-PMs at different doses. The surge of plasma testosterone levels clearly demonstrates that leuprolide is released from LeuL1 CCL-PMs in its biologically active form. The continuous stimulation of the pituitary suppresses the hypophyseal–gonadal axis (possibly through the process of down-regulation of pituitary receptors for GnRH and desensitization of the pituitary gonadotropins) and in turn the plasma testosterone levels [48], as observed in all leuprolide-treated groups. However, there was a clear difference between the duration of the effect. The plasma testosterone levels decreased by >150-fold in 24 h after i.v. injection of soluble leuprolide (0.1 mg/kg) whereas it only dropped by ca. 10-fold in 24 h after i.v. administration of LeuL1 CCL-PMs (0.13 mg/kg). Between 48 h and 120 h, the testosterone levels decreased to <0.5 ng/mL in both cases. Surprisingly, as shown in Fig. 8, testosterone peak levels were not dose-dependent yet within the same order of magnitude for all leuprolide-treated groups, indicating that a plateau-level of testosterone surge was reached already at 1.3 mg/kg dose level. The biological response pattern may be attributed to the saturation and down-regulation of the pituitary GnRH receptors by the analogue or some unknown phenomena [49]. Nonetheless, compared to soluble leuprolide, the plasma testosterone levels decreased at a substantially lower rate when formulated in LeuL1 CCL-PMs, owing to the steady and long-lasting effect of released leuprolide on plasma testosterone levels. As the aim of testosterone level determination was to examine the bioactivity of the released leuprolide rather than long-term efficacy, testosterone levels were only monitored until 120 h. In the course of the study, no clinically relevant signs were found in animals treated with LeuL1-CCL-PMs (Supplementary Table S4).

The present study reports on a novel strategy to covalently link peptides to CCL-PMs via different hydrolysable ester linkages. The small-sized and long-circulating polymeric micelle system allows sustained release of the biologically active peptide into the systemic circulation for several days following intravenous administration. Commercial products containing leuprolide such as Eligard® (gel-like depot) and Lupron depot® (microspheres) have also demonstrated good efficacy in vivo after subcutaneous or intramuscular administration [50,51]. However, the strategy we propose enables the nanoformulation to be absorbed directly in the systemic circulation following intravenous administration and allows for higher efficiency for reaching various target sites (e.g., the systemic circulation for leuprolide). Furthermore, considering the good tolerability of this nanoformulation, we believe this novel strategy has a great potential for the delivery of therapeutic peptides, especially when local administration is not feasible (e.g., due to unwanted immunogenicity induced by the absorption of peptides from the injection site).

To mention, we selected leuprolide as the model peptide and developed this delivery strategy for broad applications. This reported technology may be used to entrap not only leuprolide, but also other (hydrophobic) peptides in the micellar core to achieve higher entrapment efficiency. The use of hydrolysable linkers may allow tuneable peptide release profile at various disease sites (e.g., inflammatory and tumour tissues). Owing to the enhanced permeability and retention

(EPR) effect [53], CCL-PMs can preferentially localize into tumour and inflammatory tissues, as demonstrated in mouse melanoma model and arthritis models [24,39]. Thus these CCL-PMs may be employed for not only sustained release of therapeutic peptides in blood, but also targeting of anticancer or anti-inflammatory peptides to tumours and inflammatory sites. Altogether, these key features encourage application of this polymeric micelle system for the sustained release of a range of therapeutic peptides.

Supplementary data to this article can be found online at http://dx. doi.org/10.1016/j.jconrel.2014.12.023.

References

[1] C.L. Stevenson, Advances in peptide pharmaceuticals, Curr. Pharm. Biotechnol. 10 (2009) 122–137.
[2] A.M. Thayer, Improving peptides, Chem. Eng. News 89 (2011) 13–20.
[3] C. Borghouts, C. Kunz, B. Groner, Current strategies for the development of peptide-based anti-cancer therapeutics, J. Pept. Sci. 11 (2005) 713–726.
[4] P. Vlieghe, V. Lisowski, J. Martinez, M. Khrestchatisky, Synthetic therapeutic peptides: science and market, Drug Discov. Today 15 (2010) 40–56.
[5] M. Werle, A. Bernkop-Schnürch, Strategies to improve plasma half life time of peptide and protein drugs, Amino Acids 30 (2006) 351–367.
[6] A.W. Du, M.H. Stenzel, Drug carriers for the delivery of therapeutic peptides, Biomacromolecules 15 (2014) 1097–1114.
[7] C.S. Fishburn, The pharmacology of PEGylation: balancing PD with PK to generate novel therapeutics, J. Pharm. Sci. 97 (2008) 4167–4183.
[8] G. Gregoriadis, S. Jain, I. Papaioannou, P. Laing, Improving the therapeutic efficacy of peptides and proteins: a role for polysialic acids, Int. J. Pharm. 300 (2005) 125–130.
[9] L.L. Baggio, Q. Huang, X. Cao, D.J. Drucker, An albumin-exendin-4 conjugate engages central and peripheral circuits regulating murine energy and glucose homeostasis, Gastroenterology 134 (2008) 1137–1147.
[10] K. Uekama, H. Arima, T. Irie, K. Matsubara, T. Kuriki, Sustained release of buserelin acetate, a luteinizing hormone-releasing hormone agonist, from an injectable oily preparation utilizing ethylated beta-cyclodextrin, J. Pharm. Pharmacol. 41 (1989) 874–876.
[11] S.C. Yadav, A. Kumari, R. Yadav, Development of peptide and protein nanotherapeutics by nanoencapsulation and nanobioconjugation, Peptides 32 (2011) 173–187.
[12] M.C. Jones, J.C. Leroux, Polymeric micelles — a new generation of colloidal drug carriers, Eur. J. Pharm. Biopharm. 48 (1999) 101–111.
[13] M. Yokoyama, G.S. Kwon, T. Okano, Y. Sakurai, T. Seto, K. Kataoka, Preparation of micelle-forming polymer-drug conjugates, Bioconjug. Chem. 3 (1992) 295–301.
[14] Y. Lu, K. Park, Polymeric micelles and alternative nanonized delivery vehicles for poorly soluble drugs, Int. J. Pharm. 453 (2013) 198–214.
[15] C. Deng, Y. Jiang, R. Cheng, F. Meng, Z. Zhong, Biodegradable polymeric micelles for targeted and controlled anticancer drug delivery: promises, progress and prospects, Nano Today 7 (2012) 467–480.
[16] C. Oerlemans, W. Bult, M. Bos, G. Storm, J.F. Nijsen, W.E. Hennink, Polymeric micelles in anticancer therapy: targeting, imaging and triggered release, Pharm. Res. 27 (2010) 2569–2589.
[17] V.P. Torchilin, Multifunctional nanocarriers, Adv. Drug Deliv. Rev. 58 (2006) 1532–1555.
[18] Y. Bae, K. Kataoka, Intelligent polymeric micelles from functional poly(ethylene glycol)-poly(amino acid) block copolymers, Adv. Drug Deliv. Rev. 61 (2009) 768–784.
[19] H. Cabral, K. Kataoka, Progress of drug-loaded polymeric micelles into clinical studies, J. Control. Release 190 (2014) 465–476.
[20] C.J.F. Rijcken, C.J. Snel, R.M. Schiffelers, C.F. van Nostrum, W.E. Hennink, Hydrolysable core-crosslinked thermosensitive polymeric micelles: synthesis, characterisation and in vivo studies, Biomaterials 28 (2007) 5581–5593.
[21] M. Talelli, C.J.F. Rijcken, C.F. van Nostrum, G. Storm, W.E. Hennink, Micelles based on HPMA copolymers, Adv. Drug Deliv. Rev. 62 (2010) 231–239.
[22] R.K. O'Reilly, C.J. Hawker, K.L. Wooley, Cross-linked block copolymer micelles: functional nanostructures of great potential and versatility, Chem. Soc. Rev. 35 (2006) 1068–1083.
[23] M. Talelli, M. Iman, A.K. Varkouhi, C.J.F. Rijcken, R.M. Schiffelers, T. Etrych, K. Ulbrich, C.F. van Nostrum, T. Lammers, G. Storm, W.E. Hennink, Core-crosslinked polymeric micelles with controlled release of covalently entrapped doxorubicin, Biomaterials 31 (2010) 7797–7804.
[24] B.J. Crielaard, C.J.F. Rijcken, L. Quan, S. van der Wal, I. Altintas, M. van der Pot, J.A.W. Kruijtzer, R.M.J. Liskamp, R.M. Schiffelers, C.F. van Nostrum, W.E. Hennink, D. Wang, T. Lammers, G. Storm, Glucocorticoid-loaded core-cross-linked polymeric micelles with tailorable release kinetics for targeted therapy of rheumatoid arthritis, Angew. Chem. Int. Ed. 51 (2012) 7254–7258.
[25] M. Talelli, S. Oliveira, C.J.F. Rijcken, E.H.E. Pieters, T. Etrych, K. Ulbrich, C.F. van Nostrum, G. Storm, W.E. Hennink, T. Lammers, Intrinsically active nanobody-

modified polymeric micelles for tumor-targeted combination therapy, Biomaterials 34 (2013) 1255–1260.

[26] L. Quan, Y. Zhang, B.J. Crielaard, A. Dusad, S.M. Lele, C.J.F. Rijcken, J.M. Metselaar, H. Kostková, T. Etrych, K. Ulbrich, F. Kiessling, T.R. Mikuls, W.E. Hennink, G. Storm, T. Lammers, D. Wang, Nanomedicines for inflammatory arthritis: head-to-head comparison of glucocorticoid-containing polymers, micelles, and liposomes, ACS Nano 8 (2013) 458–466.

[27] J. Trachtenberg, The treatment of metastatic prostatic cancer with a potent luteinizing hormone releasing hormone analogue, J. Urol. 129 (1983) 1149–1152.

[28] N.J. Wojciechowski, C.A. Carter, V.A. Skoutakis, D.T. Bess, W.J. Falbe, T.R. Mickle, Leuprolide: a gonadotropin-releasing hormone analog for the palliative treatment of prostatic cancer, Drug Intell. Clin. Pharm. 20 (1986) 746–751.

[29] P.E. Lønning, E.A. Lien, Pharmacokinetics of anti-endocrine agents, Cancer Surv. 17 (1993) 343–370.

[30] P. Periti, T. Mazzei, E. Mini, Clinical pharmacokinetics of depot leuprorelin, Clin. Pharmacokinet. 41 (2002) 485–504.

[31] C.F. van Nostrum, D. Neradovic, O. Soga, W.E. Hennink, Polymeric micelles with transient stability: a novel delivery concept, Polymeric Drug Delivery I, American Chemical Society, 2006, pp. 40–54.

[32] C.J.F. Rijcken, T.F.J. Veldhuis, A. Ramzi, J.D. Meeldijk, C.F. van Nostrum, W.E. Hennink, Novel fast degradable thermosensitive polymeric micelles based on PEG-block-poly(N-(2-hydroxyethyl)methacrylamide-oligolactates), Biomacromolecules 6 (2005) 2343–2351.

[33] O. Soga, C.F. van Nostrum, A. Ramzi, T. Visser, F. Soulimani, P.M. Frederik, P.H.H. Bomans, W.E. Hennink, Physicochemical characterization of degradable thermosensitive polymeric micelles, Langmuir 20 (2004) 9388–9395.

[34] D. Neradovic, O. Soga, C.F. Van Nostrum, W.E. Hennink, The effect of the processing and formulation parameters on the size of nanoparticles based on block copolymers of poly(ethylene glycol) and poly(N-isopropylacrylamide) with and without hydrolytically sensitive groups, Biomaterials 25 (2004) 2409–2418.

[35] J. Prakash, M. Sandovici, V. Saluja, M. Lacombe, R.Q.J. Schaapveld, M.H. de Borst, H. van Goor, R.H. Henning, J.H. Proost, F. Moolenaar, G. Kéri, D.K.F. Meijer, K. Poelstra, R.J. Kok, Intracellular delivery of the p38 mitogen-activated protein kinase inhibitor SB202190 [4-(4-fluorophenyl)-2-(4-hydroxyphenyl)-5-(4-pyridyl)1H-imidazole] in renal tubular cells: a novel strategy to treat renal fibrosis, J. Pharmacol. Exp. Ther. 319 (2006) 8–19.

[36] D.K. Laimou, M. Katsara, M.T. Matsoukas, V. Apostolopoulos, A.N. Troganis, T.V. Tselios, Structural elucidation of leuprolide and its analogues in solution: insight into their bioactive conformation, Amino Acids 39 (2010) 1147–1160.

[37] S. Sundaram, C. Durairaj, R. Kadam, U.B. Kompella, Luteinizing hormone-releasing hormone receptor-targeted deslorelin-docetaxel conjugate enhances efficacy of docetaxel in prostate cancer therapy, Mol. Cancer Ther. 8 (2009) 1655–1665.

[38] D. Neradovic, W.L.J. Hinrichs, J.J. Kettenes-van den Bosch, W.E. Hennink, Poly(N-isopropylacrylamide) with hydrolyzable lactic acid ester side groups: a new type of thermosensitive polymer, Macromol. Rapid Commun. 20 (1999) 577–581.

[39] M. Coimbra, C.J.F. Rijcken, M. Stigter, W.E. Hennink, G. Storm, R.M. Schiffelers, Anti-tumor efficacy of dexamethasone-loaded core-crosslinked polymeric micelles, J. Control. Release 163 (2012) 361–367.

[40] C.J.F. Rijcken, Tuneable and degradable polymeric micelles for drug delivery from synthesis to feasibility in vivo(Thesis) Utrecht University, 2007.

[41] T. Hamaguchi, Y. Matsumura, M. Suzuki, K. Shimizu, R. Goda, I. Nakamura, I. Nakatomi, M. Yokoyama, K. Kataoka, T. Kakizoe, NK105, a paclitaxel-incorporating micellar nanoparticle formulation, can extend in vivo antitumour activity and reduce the neurotoxicity of paclitaxel, Br. J. Cancer 92 (2005) 1240–1246.

[42] M. Harada, M. Ohuchi, T. Hayashi, Y. Kato, Prolonged circulation and in vivo efficacy of recombinant human granulocyte colony-stimulating factor encapsulated in polymeric micelles, J. Control. Release 156 (2011) 101–108.

[43] T.M. Allen, C. Hansen, Pharmacokinetics of stealth versus conventional liposomes: effect of dose, Biochim. Biophys. Acta Biomembr. 1068 (1991) 133–141.

[44] J. Slager, A.J. Domb, Hetero-stereocomplexes of d-poly(lactic acid) and the LHRH analogue leuprolide. Application in controlled release, Eur. J. Pharm. Biopharm. 58 (2004) 461–469.

[45] Y. Ogawa, H. Okada, T. Heya, T. Shimamoto, Controlled release of LHRH agonist, leuprolide acetate, from microcapsules: serum drug level profiles and pharmacological effects in animals, J. Pharm. Pharmacol. 41 (1989) 6.

[46] G.W. Chodak, A critical review of maximal androgen blockade for advanced prostate cancer, Rev. Urol. 6 (2004) S18–S23.

[47] D. Weckermann, R. Harzmann, Hormone therapy in prostate cancer: LHRH antagonists versus LHRH analogues, Eur. Urol. 46 (2004) 279–284.

[48] A.V. Schally, A.M. Comaru-Schally, A. Nagy, M. Kovacs, K. Szepeshazi, A. Plonowski, J.L. Varga, G. Halmos, Hypothalamic hormones and cancer, Front. Neuroendocrinol. 22 (2001) 248–291.

[49] M.S. Frager, D.R. Pieper, S.A. Tonetta, J.A. Duncan, J.C. Marshall, Pituitary gonadotropin-releasing hormone receptors. Effects of castration, steroid replacement, and the role of gonadotropin-releasing hormone in modulating receptors in the rat, J. Clin. Invest. 67 (1981) 615–623.

[50] H. Okada, One- and three-month release injectable microspheres of the LH-RH superagonist leuprorelin acetate, Adv. Drug Deliv. Rev. 28 (1997) 43–70.

[51] O. Sartor, Eligard: leuprolide acetate in a novel sustained-release delivery system, Urology 61 (2003) 25–31.

[52] S. Jahan, S. Ahmed, N. Taqvim, Hizbullah, Possible modulation of testosterone secretion by obestatin in pubertal male rats, Pak. J. Zool. 43 (2011) 799–803.

[53] J. Fang, H. Nakamura, H. Maeda, The EPR effect: unique features of tumor blood vessels for drug delivery, factors involved, and limitations and augmentation of the effect, Adv. Drug Deliv. Rev. 63 (2011) 136–151.